Stokes friction coefficient of spherical particles in the presence of polymer depletion layers

Analytical and numerical calculations, comparison with experimental data

E. Donath,[a] A. Krabi,[b] M. Nirschl,[c] V. M. Shilov,[d] M. I. Zharkikh[d] and B. Vincent[e]*

[a] *Humboldt-University, Institute of Biology, Berlin, Germany*
[b] *MPI of Colloids and Interfaces, Berlin, Germany*
[c] *Technical University Munich, Department of Fluid Mechanics and Process Automation, Germany*
[d] *Institute of Biocolloid Chemistry, National Academy of Science of Ukraine, Kiev, Ukraine*
[e] *School of Chemistry, University of Bristol, Bristol, UK BS8 1TS*

The Stokes friction coefficient has been calculated for the case of polymer depletion near a spherical particle surface, to provide a theoretical background for the interpretation of dynamic light scattering data. In a quasi-flat Newtonian approximation an analytical solution for arbitrary viscosity profiles was obtained. Numerical integration of the Navier–Stokes equation confirmed the large range of applicability of the approximate analytical solution. Explicit equations for an exponential and a step viscosity profile are given.

To compare experiment and theory, dynamic light scattering data of liposomes with different radii in 110 kDa dextran are presented. For the first time evidence of a depletion layer relaxation effect has been obtained. This relaxation caused an effective reduction of the depletion layer thickness for small particles. A linear correction for the relaxation effect is suggested.

Particles dispersed in polymer solutions show adsorption and/or depletion phenomena.[1] If the net interaction energy of a soluble polymer with a particle surface does not outweigh the loss of configurational entropy of the polymer close to the interface a decrease in the mean polymer segment density near the interface will occur and a depletion layer is formed.[2] The hydrodynamic properties of the solution near the interface are modified in such a way, that the apparent viscosity decreases towards the interface.[3] In the approximation of local hydrodynamics, a position-dependent viscosity has been introduced.[4] If one were able to study experimentally the hydrodynamic properties of the depletion layer, valuable information on its structure and equilibrium properties could be obtained.

Generally, the thickness of the depletion layer is expected to be of the order of the polymer radius of gyration.[5–7] Even for large molecular weight polymers this distance is quite small as compared with the dimensions of most colloidal particles. This makes it very difficult to determine the depletion effect from rheological measurements, since the effect of the reduced viscosity on hydrodynamic drag coefficients should be of the order of the ratio of polymer radius to particle radius. A surprisingly large effect of the depletion layer, however, has been observed in electrokinetic experiments,[8,9] where the electrophoretic mobility of particles at a given polymer concentration was up to several times larger than expected from the bulk viscosity. This was explained by the specific flow velocity field around a charged particle moving under the influence of an electric field in a polymer solution which obeys potentiality except inside the range of the electric double layer. As a consequence the electrophoretic mobility depends solely on the viscosity in the range of the electric double layer and not on the bulk polymer solution viscosity.[10]

A more detailed theoretical analysis showed that an integral over the electric field strength weighted viscosity determined the electrokinetic depletion effect.[11] The electric potential in the diffuse part of an electric double layer can be approximately described by an exponential decay, with the Debye length as the characteristic decay parameter. This has the consequence that the viscosity, at larger distances from the particle surface, cannot be obtained with sufficient accuracy, given the inevitable experimental scatter in electrokinetic experiments. However, an estimation of the apparent viscosity in the immediate vicinity of the interface from electrokinetic experiments in the range of higher salt concentrations is possible.[12] Generally, detailed information on the viscosity profile is not available, because the electrokinetic effect of polymer depletion represents an integral measure of the hydrodynamic depletion influence.

Modern techniques of dynamic light scattering allow for sufficiently precise measurements of the diffusion coefficient of small particles.[13] Provided that the particles can be considered as hard spheres, the Einstein–Perrin equation allows calculation of the particle radius from the diffusion coefficient. Since it is possible to measure diffusion coefficient changes as small as a few per cent the detection of depletion effects, at least for small particles, should be possible.

Recently, various viscosity profiles were used to quantitatively explain depletion layer effects of dextran on the electrophoretic mobility of liposomes.[11] The Stokes radius as a function of polymer concentration was measured at the same time by means of dynamic light scattering. To date, a theoretical expression for the Stokes friction coefficient in the presence of a depletion layer has not been available. Below we provide an analytical approximation and compare it with a numerical solution of the problem. Special attention is paid to the question as to whether, in contrast to electrokinetic experiments, the viscosity at larger distances can be assessed.

A comparison with experimental data further showed that, in situations where dynamic light scattering can be used to determine depletion effects, the time of formation of the depletion layer is of crucial importance for the interpretation of experiments. As a consequence, relaxation effects of depletion layer formation have to be incorporated into both flocculation and electrokinetic concepts.

Analytical solution

Let us introduce local Cartesian coordinates to describe the liquid flow with a velocity, v, through a thin layer with a reduced viscosity, $\eta(x)$. The x-axis is directed perpendicular to the particle surface and the y-axis parallel to the liquid velocity.

The viscosity profile, $\eta(x)$ is given by:

$$\eta(x) = \eta_P f(x) \tag{1}$$

where η_P is the bulk viscosity of the polymer solution.
The tangential tension, σ_t, in a quasi-flat system is constant,

$$\sigma_t = \eta \frac{dy}{dx} = \eta_P \frac{dv_0}{dx} \tag{2}$$

where v_0 denotes the bulk liquid velocity distribution outside the depletion layer. The velocity gradient within the depletion layer can be expressed by the bulk velocity gradient substituting eqn. (1) into eqn. (2):

$$\frac{dv}{dx} = \frac{1}{f(x)} \frac{dv_0}{dx} = \left(\frac{1}{f(x)} - 1\right) \frac{dv_0}{dx} + \frac{dv_0}{dx} \tag{3}$$

Integration of eqn. (3) yields:

$$\begin{aligned} v(x) &= \int_0^x \frac{dv}{dx_1} dx_1 \\ &= \frac{dv_0}{dx} \int_0^x \left(\frac{1}{f(x_1)} - 1\right) dx_1 + \frac{dv_0}{dx} x \\ &= K\sigma_t + v_0 \end{aligned} \tag{4}$$

K is given by:

$$K = \frac{1}{\eta_P} \int_0^\infty \left(\frac{1}{f(x)} - 1\right) dx \tag{5}$$

Next, the hydrodynamic boundary conditions at the particle surface with a depletion layer have to be modified as follows:

$$\begin{aligned} v_n|_{r=a} &= 0 \\ v_t|_{r=a} &= K\sigma|_{r=a} \end{aligned} \tag{6}$$

Let us now explore the influence of the modified boundary conditions (6) on the Stokes' drag coefficient. We calculate the drag force, that a particle with a depletion layer experiences in a homogeneous liquid flow.

The general solution for a creeping axisymmetrical flow in spherical coordinates, Θ, r, has the following form:[14]

$$\begin{aligned} v_r &= \cos\Theta\left(U_\infty + \frac{B}{r^3} + \frac{C}{r}\right) \\ v_\Theta &= -\sin\Theta\left(U_\infty - \frac{B}{2r^3} + \frac{C}{2r}\right) \end{aligned} \tag{7}$$

where B and C are constants. The liquid velocity at infinite distance from the particle surface is U_∞ and the force exerted on the particle equals:

$$F = 4\pi\eta C \tag{8}$$

The tangential tension in spherical coordinates has the form:

$$\sigma_{r_\Theta} = \eta\left(\frac{1}{r}\frac{\partial v_r}{\partial\Theta} + \frac{\partial v_\Theta}{\partial r} - \frac{v_\Theta}{r}\right) \tag{9}$$

Substituting eqn. (7) into eqn. (6) and taking into account eqn. (9), we obtain a system of linear equations:

$$\begin{aligned} U_\infty + \frac{B}{a^3} + \frac{C}{a} &= 0 \\ U_\infty - \frac{B}{2a^3} + \frac{C}{2a} &= \frac{\eta_P K}{a}\frac{3B}{a^3} \end{aligned} \tag{10}$$

where a is the particle radius. The solution of this system of equations is:

$$C = -\frac{3}{2} U_\infty a \frac{\left(1 + 2\frac{\eta_P K}{a}\right)}{\left(1 + 3\frac{\eta_P K}{a}\right)} \tag{11}$$

And, finally, the correction to the Stokes coefficient, f_c, for a changed viscosity in a thin layer around the spherical particle becomes:

$$f_c = 6\left(\frac{1 + 2\frac{\eta_P K}{a}}{1 + 3\frac{\eta_P K}{a}}\right) \tag{12}$$

If K tends to infininity, $f_c = 4$. This coincides with limiting value of the Hadamard–Rybchinskij equation for the drag coefficient of a gaseous bubble.[15] In this case the tangential tension on the particle surface becomes zero.

Let us next provide an explicit solution of eqn. (12) for the previously used[11] exponential and double-step viscosity profiles, eqn. (13) and (14):

$$\eta(x) = \frac{\eta_P}{1 + \left(\frac{\eta_P}{\eta_0} - 1\right)\exp(-x/\lambda)} \tag{13}$$

$$\eta(x) = \begin{cases} \eta_S & x \leqslant \lambda_1 \\ \eta^* & \lambda_1 \leqslant \lambda_1 + \lambda_2 \\ \eta_P & x > \lambda_1 + \lambda_2 \end{cases} \tag{14}$$

The various λ coefficients denote the thickness parameters in the above viscosity profiles. In eqn. (13) η_0 is the viscosity at $x = 0$. η_S and η^* are the heights of the two steps in the step viscosity profile (14).

For the exponential profile (13), as well as the double-step profile (14), the modified Stokes' drag coefficients are provided in eqn. (15) and (16), respectively.

$$f_c = 6\frac{1 + 2\frac{\lambda}{a}\left(\frac{\eta_P}{\eta_0} - 1\right)}{1 + 3\frac{\lambda}{a}\left(\frac{\eta_P}{\eta_0} - 1\right)} \tag{15}$$

$$f_C = 6\frac{1 + \frac{2}{a}\left[\left(\frac{\eta_P}{\eta_S} - 1\right)\lambda_1 + \left(\frac{\eta_P}{\eta^*} - 1\right)\lambda_2\right]}{1 + \frac{3}{a}\left[\left(\frac{\eta_P}{\eta_S} - 1\right)\lambda_1 + \left(\frac{\eta_P}{\eta^*} - 1\right)\lambda_2\right]} \tag{16}$$

Numerical integration

For the numerical solution, the Navier–Stokes and the continuity equation of an incompressible fluid in their integral form may be used:

$$\int_S\int \boldsymbol{p}\, d\boldsymbol{A} = \int_S\int \tau\, d\boldsymbol{A} \tag{17}$$

$$\int_S\int \boldsymbol{v}\, d\boldsymbol{A} = 0 \tag{18}$$

where p is the hydrodynamic pressure and τ is the viscous stress tensor.

This type of equation can be solved numerically with a

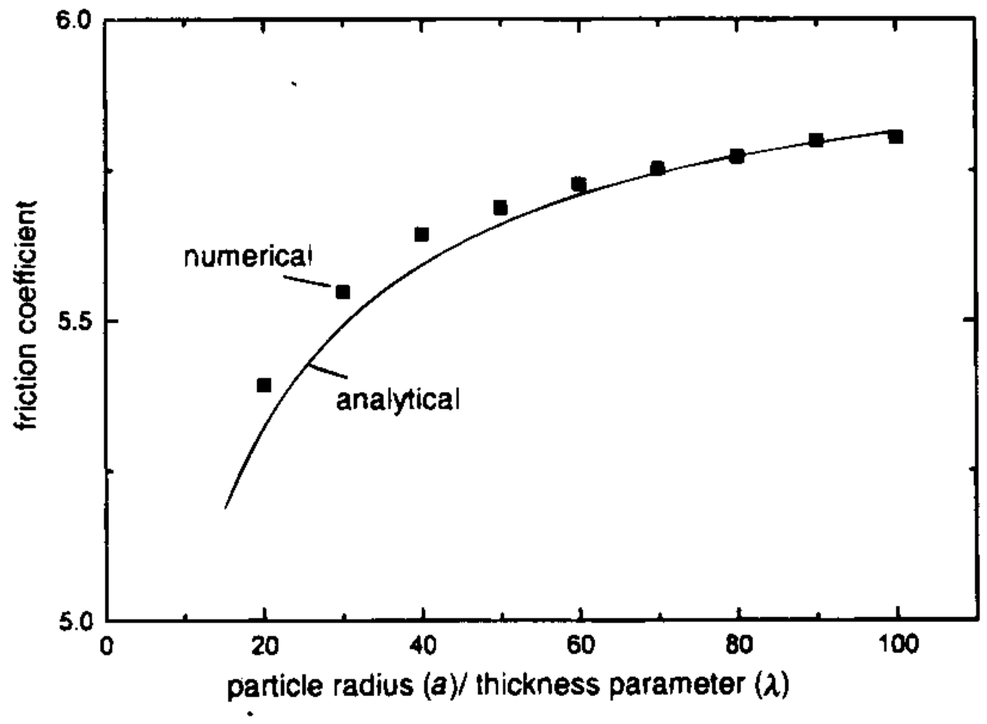

Fig. 1 Stokes friction coefficient in the presence of a polymer depletion layer as a function of the effective thickness of the depletion layer. The solid curve corresponds to an analytical solution for the Stokes coefficient with an exponential viscosity profile according to eqn. (15) with $\eta_P = 0.003965$ and $\eta_0 = 0.0009$ Pa s. (■) are numerical calculations for the same viscosity profile.

finite volume formulation, where the geometry of the spherical particle is described by curvilinear coordinates, one radial and one circumferencial over the particle surface. An axisymmetric mesh is generated around the spherical particle where the force balance is then approximated on the four sides dA around one grid point. The discretization leads to a system of tridiagonal matrices.

The numerical solution procedure is described in detail in ref. 16–18 and will only be briefly outlined in this paper. The two velocity components are propagated in time using an implicit predictor/corrector scheme along alternating coordinate directions. The pressure change or correction algorithm consisted of solving a Poisson equation derived from the continuity equation. The Poisson equation can also be solved by the predictor/corrector scheme. Alternatively, a direct solver can speed up the solution procedure of the computations by a factor of two. The scheme was originally developed for the calculation of non-stationary flow conditions. So the time-dependent acceleration has been introduced into the solution procedure. During the iterations of the momentum and the Poisson equation this term approaches zero for the steady-state solution.

In this work we have used second-order central differences everywhere in space and backward Euler scheme for the time. The accuracy of the calculated results depends on the number of iterations. Usually 1000 iterations are necessary to converge the sytem with an accuracy of 1% . This can be performed on an Alpha workstation within 90 min computational time.

The drag coefficient c_d is approximated by integrating the pressure and viscous forces over the particle surface. The relationship between the drag coefficient and the friction coefficient, f_c, is given by:

$$f_c = \frac{2c_d \rho U_\infty a}{4\eta_P} \tag{19}$$

where ρ is the density of the fluid.

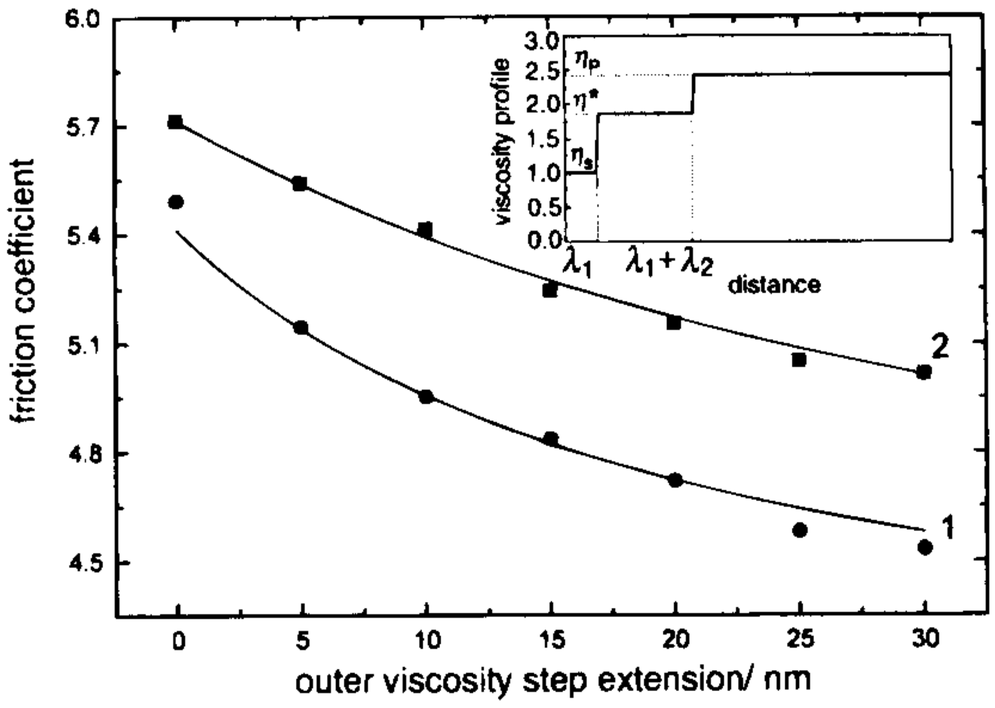

Fig. 2 Stokes friction coefficient as a function of the outer viscosity step extension, λ_2, for particle radii: 1, 25 nm and 2, 50 nm. The solid curves are analytical solutions with a double-step viscosity profile according to eqn. (16) with $\lambda_1 = 0.8$ nm, $\eta_P = 0.003965$ Pa s, $\eta_S = 0.00089$ Pa s and $\eta^* = 0.002735$ Pa s. The double-step viscosity profile is shown in the insert. (■) and (●) are the corresponding numerical calculations.

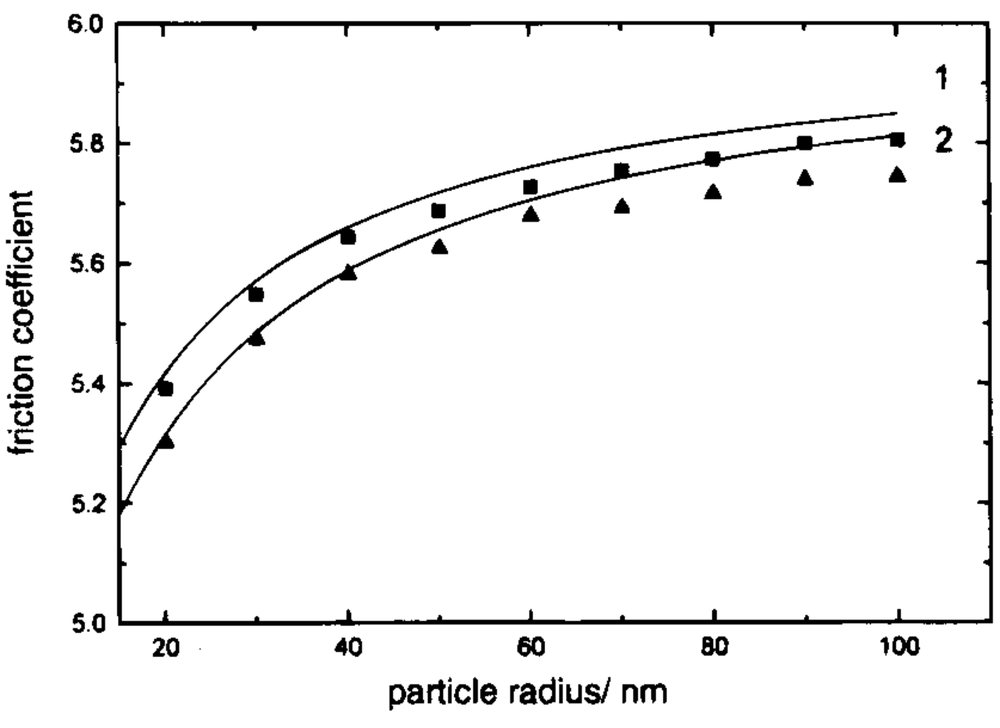

Fig. 3 Friction coefficient as a function of the particle radius for two different viscosity profiles. 1, exponential viscosity profile [eqn. (15)] with $\lambda = 0.8$ nm, $\eta_P = 0.003965$ Pa s, $\eta_0 = 0.00089$ Pa s. 2, step profile [eqn. (16)] with $\lambda_2 = 0$, $\lambda_1 = 1$ nm, $\eta_P = 0.003965$ Pa s, $\eta_S = 0.00089$ Pa s. (■) Numerical calculations for the exponential viscosity and (▲) numerical calculations for the step profile.

Theoretical results

Let us first compare the analytical and numerical solution. Because the analytical solution provided in eqn. (12), together with eqn. (5), was derived under the limitation of a quasi-flat system it is important to study the deviation between the analytical and the numerical solution as a function of the 'ratios particle radius to thickness of the depletion layer'. This is done in Fig. 1 and 2. In Fig. 1 the theoretical friction coefficient for an exponential viscosity profile in the depletion layer [eqn. (13)] is compared with the numerical solution. It is obvious that the analytical solution almost matches the numerical one, except in the region of relatively thick depletion layers. Here, the analytical solution overestimates the effect of depletion on the friction coefficient, but only by a few per cent. It is clear that neglecting the curvature of the surface in the analytical solution should always result in an overestimation of the depletion effect.

It is remarkable that, in general, the depletion effect is relatively large. For example, even if the depletion layer thickness is only 1/20 of the particle radius, the friction coefficient is reduced by 1/6, almost 30% of the theoretical limit. This can be attributed to the large increase in the flow velocity within the depletion layer, due to the decreased viscosity close to the particle interface approaching the solvent viscosity at the surface while the bulk viscosity was larger by a factor of four. The hydrodynamic flow was 'focused' onto the particle surface.

As mentioned in the Introduction it is important to consider the situation when the viscosity outside the diffuse part of the double layer is still smaller than the bulk value. While in electrokinetic experiments this viscosity reduction outside the double layer is not measurable, in principle, the situation is quite different for diffusion.

The simplest way to model an unknown monotonic viscosity profile was to assume a double-step of the viscosity, as shown in the insert, where the first small step was identical to the step we derived from electrokinetic experiments.[11] It is of interest to consider how much the hydrodynamic depletion effect depends on the extension of the second outer step. As

shown in Fig. 2, the friction coefficient decreased monotonically with increasing extension of the depletion layer. (To provide an analytical limiting value is not meaningful since the analytical solution does not apply to very thick depletion layers.) Again, the analytical and numerical solutions were close. It is clear that the small scatter in the numerical curves originated from difficulties in handling the step profile with a limited number of grid points.

Although both the hydrodynamic and the electrokinetic effects are given by integrals over the inverse of the viscosity profile [eqn. (5) and eqn. (4) in ref. 11], it is clear that, since the electrokinetic effect is additionally weighted by the electric field strength, both estimates reflect different aspects of the rheology inside the depletion layer. This is demonstrated in Fig. 3 where an exponential profile is compared with a single-step profile. Both profiles yielded close fits of electrokinetic data (Fig. 8 in ref. 11) while they separate into two different curves in Fig. 3. The deviation of the numerical solution from the analytical formula in the step profile is again attributed to difficulties of handling a step profile in a grid scheme.

As expected, the theoretical resolution of the hydrodynamic estimation of the depletion layer viscosity profile increase with decreasing particle radius.

Discussion and comparison with experimental data

It has been demonstrated theoretically that the reduced viscosity in a depletion layer should result in a measurable large decrease in the Stokes friction coefficient, provided that the particles are small enough. An analytical expression for the friction coefficient in the presence of a depletion layer was derived and verified numerically. It has also been shown that the electrokinetic and the hydrodynamic characterisation of the depletion layer may provide mutually supporting information concerning hydrodynamic properties of the polymer depletion layer.

The use of continuum hydrodynamics is an approximation, the validity of which has to be discussed before drawing conclusions regarding the depletion effect. Generally, continuum hydrodynamics require the structural inhomogeneities of the solution to be much smaller than the characteristic length of flow change. This is certainly not the case for the depletion layer where, over the molecular dimensions of the polymers, a significant velocity gradient is present. On the other hand, the particular question of determining the diffusion coefficient is associated with flow averaging over a time interval of the order of 10^2–10^3 s. Within this time, the individual positions of the polymers in the depletion layer are smeared out, thus giving rise to an average of the segment density profile, the mean hydrodynamic properties of which, we think, can be adequately described by a mean viscosity profile. This is further justified by the consideration that the characteristic time of flow relaxation is much smaller than polymer and particle diffusion. This ensures instantaneous hydrodynamic interaction between the polymers and between the polymers and the particle surface. Nevertheless, in future, improved theories should explicitly consider non-local viscosity effects in order to arrive at a quantitative description of the viscosity profile and its influence on interfacial hydrodynamics. Within the scope of this study the use of an averaged viscosity profile seems to be sufficient, especially, in view of the further difficulties explained below.

Another point worth discussing is the neglect of the non-Newtonian behaviour of the polymer solution. While, generally, under the influence of external forces, provided the shear is large enough, polymer solutions show non-Newtonian behaviour, it has to remembered that in the case of particle diffusion in a polymer solution it is the intrinsic thermal motion driving the polymers and particles. The quasi-flat approach of calculating the friction coefficient required the colloidal particles being much larger than the polymer radius of gyration.This is equivalent to a polymer thermal motion much more intense than the particle diffusion. Consequently, the shear stress acting upon the polymers is weak and slowly changing as compared to the polymer diffusion. Thus, it seems to be a fair assumption not to consider non-Newtonian behaviour in the case of large particles diffusing in polymer solutions.

However, there are further major problems which complicate the direct comparison of electrokinetic and diffusion experiments with polymer depletion layers at particle surfaces. First, as demonstrated above, it is not possible to measure the decrease of the friction coefficient in the presence of a depletion layer if the particles are large as compared to the depletion layer thickness. On the one hand, the precision of the light scattering experiments decreases with increasing particle radius and increasing bulk viscosity because the diffusion coefficient becomes too small. In parallel, the depletion induced reduction of the friction coefficient is also small if the particles are large.

Secondly, whenever polymer depletion is present, depletion flocculation has to be taken into account. Since precise dynamic light scattering experiments require measuring times of at least several minutes it might be difficult to avoid artificial aggregation effects.

Another difficulty, not investigated in this paper, is associated with the applicablity of the currently available electrokinetic theory of depletion. Although, recently, non-linearity and arbitrary viscosity profiles have been considered, the theory is limited to large particles as compared to the double-layer thickness. This general discrepancy between the ranges of applicability of both methods with regard to the particle size may cause serious problems in practice since it might be difficult to produce particles of the required different sizes with identical surfaces. Moreover, the electrokinetic characterization is possible only with sufficiently charged particles. The charge should also not depend on the bulk polymer concentration.

We were able to overcome these problems using liposomes of different sizes produced by an extrusion technique. Details of the preparation are given in ref. 11. The liposome charge is given by the percentage of charged lipid. The charge was adjusted to guarantee electrostatic stabilization in the light scattering experiment. Fig. 4 shows a typical example of the

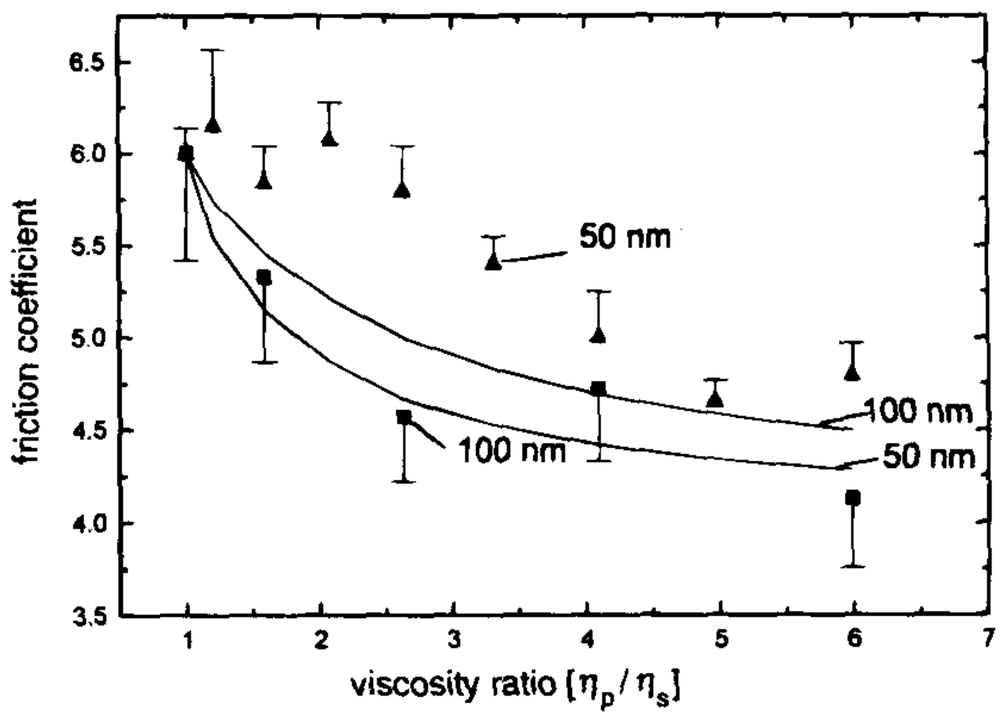

Fig. 4 Friction coefficient as a function of the viscosity ratio η_P/η_S. The solid lines are theoretical plots according to a single-step profile with a characteristic thickness of the depletion layer $\lambda = 10$ nm. Particle radius (a): 1, 10 nm and 2, 50 nm. The solid points are experimental results from dynamic light scattering on liposomes from L-α-lecithin, containing 20% phosphatidylserine in 10 mM KCl electrolyte solution. The dextran solutions with the appropriate concentrations were prepared and some liposome stock solution was added for a good scatter signal. (▲) liposomes, prepared with a nuclepore filter of 50 nm pore size. (■) liposomes prepared with 100 nm pore size. Error bars are the S.D.

measured friction coefficient decrease calculated from the diffusion coefficient. Two particle sizes with mean radii of *ca.* 25 and 50 nm were employed. Dextran of 110 kDa molecular weight formed the depletion layer. Consequently, a depletion layer thickness given by the radius of gyration of the dextran molecules (*ca.* 10 nm) was expected. The two solid lines are the theoretical plots of the depletion effect, assuming a depletion layer thickness of the order of the polymer radius of gyration.

While, in general, the measured depletion effect was in the range of the theoretical predictions and showed an increase with increasing bulk polymer viscosity (decrease of the friction coefficient), to our surprise the hydrodynamic depletion effect was larger for the larger particles contrary to the theoretical predictions. With the smaller particles a decrease of the friction coefficient started to be visible at polymer to solvent viscosity ratios of *ca.* 3. At higher polymer viscosities the friction coefficient of the smaller particles came close to that of the larger particles.

In these measurements, special attention was paid to the problem that the polymer molecules in the measuring solution also contributed to the fluctuating light scattering signal. The CONTIN algorithm used for the calculation of the size distribution from the autocorrelation function was able to resolve clearly both size distributions, *i.e.* of the liposomes and of the polymers. The result did not depend on variation of the scattering angle and on variation of the sampling time. Moreover, if the polymer signal would have interfered with the light scattering signal from the particles, apparent smaller friction coefficients for the smaller particles would have resulted. Since the observed effect is the opposite, the idea of an artificial, polymer-particle light-scattering interference may be ruled out.

What can be the reason for this inversion with regard to the particle size of the depletion effect? It is clear that for the relatively small particles the Brownian motion of the particle itself cannot be neglected when discussing the formation of a depletion layer. It is likely that the time necessary to approach the equilibrium segment density distribution in the depletion layer for small particles is large, compared with the mean time the particle takes to diffuse over a distance comparable to the thickness of the depletion layer. A depletion layer relaxation effect is expected consisting in an incomplete formation of the depletion layer for smaller particles.

As a first approach a linear correction for the friction coefficient, f_c^{relax}, can be expressed as follows:

$$f_c^{relax} = f_c + \frac{1}{1 + \frac{\tau_{part}}{\tau_{pol}}} (6 - f_c) \qquad (20)$$

Here, τ_{pol} is the characteristic time of formation of the equilibrium depletion layer while τ_{part} is the time the particles needs to diffuse over a distance comparable to the characteristic thickness of the depletion layer, $\tau_{part} \sim 1/\eta_p a$. As eqn. (20) shows, if the formation of the depletion layer is infinitely slow no depletion is present. At present not very much is known about τ_{pol}. A lower boundary might be the diffusion time of the polymer over the distance of the depletion layer, which would be proportional to $1/\eta_s r_g$, where r_g is the radius of gyration of the polymer. On the other hand, the particle mostly experiences the polymer bulk viscosity. From these considerations it is clear that, with increasing bulk viscosity, the relaxation effect becomes smaller. Increasing particle size would also decrease the relaxation effect. This is in qualitative agreement with the experimental data reported here. For the smaller particles of 25 nm radius these assumptions lead to a theoretical correction coefficient of 0.13 for 4% w/w dextran. The experimental value was significantly larger. Consequently, the formation time of the depletion layer has to be larger than the pure diffusion time. Increasing τ_{pol} by a factor of ten yielded a correction coefficient of 0.6, closer to the experimental data. This can be understood considering the fact that, for probing the equilibrium structure near an interface, a number of polymer conformations have to be averaged. To understand quantitatively the depletion layer relaxation effect the kinetics of formation of the layer have to be worked out on the basis of non-equilibrium statistical mechanics which is beyond the scope of this paper.

It can be further argued that, at least in the presence of fluid membranes, the undulating, thermal movement of the particle surface contributes to the depletion layer formation kinetics. Finally, the larger the curvature of the particle the smaller the depletion effect. In our case this also might be of importance.

In summary, it is clear that further investigation of this possible relaxation effect is of major importance, not only in determination of the friction coefficient but also in almost all other phenomena depending on the depletion layer, such as electrophoresis or flocculation studies, whenever small particles with a sufficiently large diffusivity are involved.

We are grateful for the support of the DAAD-ARC exchange programme and for support from INTAS.

References

1 G. J. Fleer, J. M. H. M. Scheutjens, M. A. Cohen Stuart, T. Cosgrove and B. Vincent, *Polymers at Interfaces*, Chapman and Hall, London, 1993.
2 R. I. Feigin and D. H. Napper, *J. Colloid Interface Sci.*, 1980, **75**, 525.
3 H. Müller-Mohnssen, D. Weiss and A. Tippe, *J. Rheol.*, 1990, **34**, 223.
4 H. Bäumler and E. Donath, *Stud. Biophys.*, 1987, **120**, 113.
5 F. K. Li-in-on, B. Vincent and F. A. Waite, *J. Colloid Interface Sci.*, 1987, **116**, 305.
6 S. Emmett and B. Vincent, *Phase Transitions*, 1990, **21**, 197.
7 G. J. Fleer, J. M. H. M. Scheutjens and B. Vincent, in *Polymer Adsorption and Dispersion Stability*, ed. E. D. Goddard and B. Vincent, ACS Symp. Ser. 240, 245, American Chemical Society, Washington, DC, 1984.
8 D. E. Brooks and G. V. F. Seaman, *J. Colloid Interface Sci.*, 1973, **43**, 670.
9 H. Bäumler, E. Donath, L. Pratsch and D. Lerche, in *Hemorheologie et Agregation Erythrocytaire*, ed. J. F. Stoltz, M. Donner and A. L. Copley, Editions Medicales Internationales, Cachan Cedex, 1991, p. 24.
10 E. Donath, P. Kuzmin, A. Krabi and A. Voigt, *Colloid Polym. Sci.*, 1993, **271**, 930.
11 E. Donath, A. Krabi, G. Allan and B. Vincent, *Langmuir*, 1996, **12**, 3425.
12 H. Bäumler, E. Donath, A. Krabi, W. Knippel, A. Budde and H. Kiesewetter, *Biorheology*, in the press.
13 N. Ostrowsky, *Chem. Phys. Lipids*, 1993, **64**, 45.
14 G. Happel and H. Brenner, *Low Reynolds Numbers Hydrodynamics*. Nijhoff, The Hague, 1983.
15 L. D. Landau and E. M. Lifschitz, *Lehrbuch der Theoretischen Physik, Hydrodynamik*, Akademie-Verlag, Berlin 1981, p. 77.
16 H. Nirschl, *VDI Fortschrittberichte*, 1994, **7**, 248.
17 H. Nirschl, H. A. Dwyer and V. Denk, *J. Fluid Mech.*, 1995, **283**, 273.
18 H. Nirschl, H. A. Dwyer and V. Denk, A Chimera grid scheme for the calculation of particle flows, AIAA 94-0519, 1994.

Paper 6/03103J; *Received* 2nd *May*, 1996